Chapter 27
An Energy-Based Approach Towards Liquefaction Potential Analysis: Agartala City

Abhileen Chatterjee and **Sima Ghosh**

Introduction

Soil Liquefaction can be described as a natural phenomenon occurring when the induced shear strain increases the pore water pressure in the soil resulting in loss of shear strength and bearing capacity of the soil. Liquefaction failures are primarily categorized into two broad heads—(i) Flow Failures and (ii) Cyclic Mobility. Flow failures occur in response to static shear stresses coming from mostly overlying superstructures on loose sands. When the static shear stress exceeds the shear strength of the underlying saturated cohesionless soil layer, the soil starts to flow, causing settlements and failure of the infrastructure. On the contrary, cyclic mobility occurs due to repeated loadings such as earthquakes and is considered to be more common than flow failures.

Seed and Idriss [17] mentioned that soil response is a function of increasing pore water pressure due to cyclic loading. Bozorgnia and Bertero [4] supports the conventional fact that generation of pore pressure in saturated soils is firmly associated with strain amplitude than the stress amplitude. Due to parallel complexities determining strain amplitudes in soil, a theory was developed by Nemat-Nasser and Shokooh [14], which relates densification of drained soils and pore pressure generation in undrained cases to the dissipated energy. Arias [3] studied ground shaking and characterized response based on a parameter involving seismic energy evaluated from recorded ground acceleration, velocity, or displacement time histories. The gross energy consumed by a group of oscillators with single degrees of freedom (SDOF) was represented as a ground motion parameter known as the Arias Intensity. Kayen and Mitchell [10] devised a methodology to evaluate the liquefaction potential of a site employing Arias Intensity. An aspect of the superiority of that method over

---

A. Chatterjee (✉) · S. Ghosh
Department of Civil Engineering, National Institute of Technology Agartala, Tripura, India
e-mail: abhileen96@rnd.iitg.ac.in

the stress-based approach is the obliteration of the Magnitude Scaling Factor (MSF) because Arias Intensity itself consists of the amplitude, duration, and frequency content of the earthquake motion.

In this paper, an earthquake has been considered to characterize the liquefaction loading, recorded on 3rd January 2017, at 09:09:0.5 UTC [1]. A moderate moment magnitude of $M_W = 5.6$ was recorded as per GCMT data, and a Modified Mercalli Intensity (MMI) of IV was reported at various cities in Tripura, including Agartala. The epicentre was located near the Tripura-Mizoram border possessing coordinates of 23.98°N and 92.03°E, and the hypocentral depth was estimated to be 24.5 km.

Characterizing the Liquefaction Loading

Arias Intensity is calculated from two orthogonal accelerograms and is mathematically given as below:

$$I_h = \frac{\pi}{2g}\left[\int_0^{t_0} a_x^2(t)dt + \int_0^{t_0} a_y^2(t)dt\right] \tag{27.1}$$

Here t_0 is the strong motion duration. This paper considers the x- and y- components of the acceleration time history of the scenario earthquake as given in Fig. 27.1 [1]. The acceleration time histories adopted for this study is seen to be irregular ground motion signals depicting fluctuation of ground acceleration with temporal variation. For the ease of calculation of Arias Intensity for the concerned earthquake event, a smooth equivalent dynamic load has been considered from the given time history.
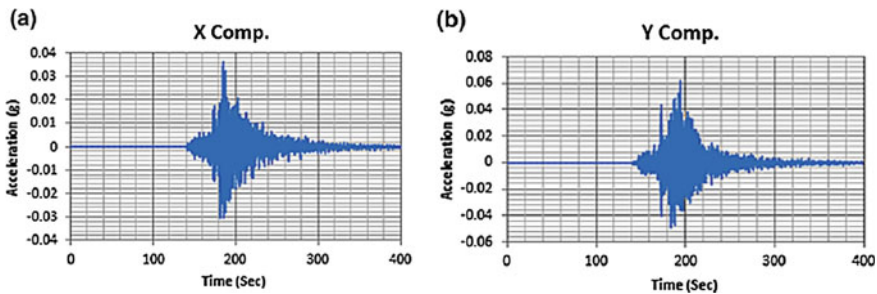

Fig. 27.1 The plot of acceleration—time history of the scenario earthquake, **a** X—Component Plot, **b** Y—component Plot [1]

Equivalent Dynamic Load

For ease of calculations, the paper assumes that similar deformations are experienced due to a uniformly varying load from the irregular earthquake loading. Seed and Idriss [16] claimed that the mean acceleration is almost similar to 0.65 times the Peak Ground Acceleration (PGA). The significant cycle (NS) count varies with the earthquake magnitude. Lee and Chan [12] gave a procedure for the irregular acceleration time history to be transformed into an equivalent no. of cyclic shear stress cycles having Maximum Magnitude $= k - M_W$ (where k is a constant and $k < 1$). The conversion parameters for each cycle have been adopted from the chart produced by Seed et al. (1975). The number of equivalent cycles for the x- and y- components of the accelerogams are evaluated to be 7.2 and 4.3, respectively.

Calculation of Arias Intensity at Surface

In this context, to evaluate the equations of motion for each of the acceleration component peak ground acceleration plays an important role. Mog et al. [1] specifies that the ground motion records are acquired from the North East Institute of Science and Technology (NEIST), India which is located at an approximate distance of 297 km from the estimated epicentre. Since Fig. 27.1b depicts the maximum value of peak ground acceleration to be around 0.064 g at a distance of 297 km, it is evident that studies specific to target regions are necessary for design of buildings and disaster management. Youd et al. [22] while answering some of the questions regarding selection of peak ground acceleration noted that $a_{\max}$ can be evaluated from accelerograms. It has also been suggested to take up a group of earthquake records with compatible magnitudes.

In Neo-deterministic seismic hazard analyses, earthquakes of magnitudes greater than 5 are considered from synthetic records developed from geophysical and geotechnical aspects of the site. That said, the study takes up the Design Ground Acceleration (DGA) formulated by Parvez et al. [15] using Neo-deterministic analysis approach based on the natural frequencies of infrastructure. It has been found that the DGA values in the proximity of Tripura region varies from 0.36 to 0.6 g. DGA being analogous to peak ground acceleration with an added advantage of frequency content of neighbouring infrastructures, is safe to use for this study. Mog et al. [1] estimates the maximum spectral acceleration to be 0.25 g at a distance of 297 km and considering the frequency parameter designated for the infrastructures in Agartala area, a peak ground acceleration value of 0.4 g has been adopted for this study.

Employing Eq. (27.1) the Arias Intensity at the surface has been calculated using the acceleration parameters from the earthquake records. The integration has been performed in Matlab to safeguard any human error using the traditional trapezoidal rule. The number of steps for the calculation has been kept to be 1000 for precise results and the integration over total ground shaking duration of 3 s [1] gives us the

surface Arias Intensity ($z = 0$) to be 1.25 m/s. Analogous to that in stress-based approach, this methodology takes into account a factor that addresses the influence of depth on the Arias intensity. It is called the Burial Reduction Factor (r_b) which when multiplied with the Arias intensity at the surface, produces the equivalent Arias Intensity generated due to the earthquake of a given magnitude at the desired depth where liquefaction potential is to be evaluated. Mathematically, r_b is given as in Eq. (27.2) below.

$$r_b = \exp\left[\frac{35}{(M_W)^2} \times \sin(-0.09 \times z)\right] \qquad (27.2)$$

Here z is the critical depth of liquefaction and the term ($-0.09 \times z$) is in radians. Now, the Arias intensity at the depth z, also known as the demand produced during the earthquake event is denoted by $I_{h,\text{eq}} = I_h(z) = r_b \times I_h(z = 0)$.

Characterizing the Resistance to Liquefaction

Liquefaction Resistance is generally demonstrated in terms of similar parameters as used for the loading to be characterized. In the case of the traditional stress-based approach, the liquefaction resistance is expressed in terms of Cyclic Resistance Ratio (CRR), which can be illustrated as the cyclic stress ratio that initiates liquefaction. In this approach, the resistance to liquefaction is calculated in terms of requisite Arias Intensity for the initiation of the phenomenon. This paper attempts to determine the liquefaction resistance using Standard Penetration Test (SPT) data from different subsurface layers at the target region. A sample BH- 02 (Table 27.1) at Gandhi Ghat, Agartala [23.8274° N, 91.2758° E], has been taken up to account for the subsurface calculations, as shown later in this paper.

Figure 27.2a–c show the variation of SPT N-count, fine content of each soil layer at the target site and the corrected SPT $(N_1)_{60,CS}$ variation with incremental depth below the ground level.

Susceptibility Criteria

Soils demonstrating sand-like, clay-like or intermediate behaviour were categorized by Boulanger and Idriss [5] based on behavioural patterns of fine-grained soils under monotonic and cyclic undrained loading on the basis of consistency limits. Behavioural consistency for samples of cyclic test data from that site was calculated taking into account the collations of stress–strain loops and ratios of excess pore water pressure. Andrews and Martin [2] proposed liquefaction susceptibility criteria of clayey and silty soils based on their liquid limits and clay content, i.e. the weight of grains finer than 0.002 mm. Three general possibilities are proposed considering

Table 27.1 Soil Profile of a sample borehole (BH-02) at Gandhi Ghat within Agartala city

| Thickness (m)	Layers	γ_b (kN/m³)	LL	PL	G	w_n	N-values
0.8	Filled up brown sand	17.7	25.50	21.47	2.66	29.54	2
3.3	Dark grey soft sandy clayey silt	19.0	-	-	2.66	28.45	15
2.10	Light brownish fine to medium sand	18.5	32.50	21.07	2.65	42.68	12
4.3	Light grey soft to medium silty clay / clayey silt	15.6	-	-	2.40	108.66	6
4.85	Blackish grey soft decomposed wood grass mixed up with silty clay	18.8	42.50	25.67	1.88	44.15	5
4.65	Light grey firm soft silty clay	17.7	25.50	21.47	2.66	29.54	2
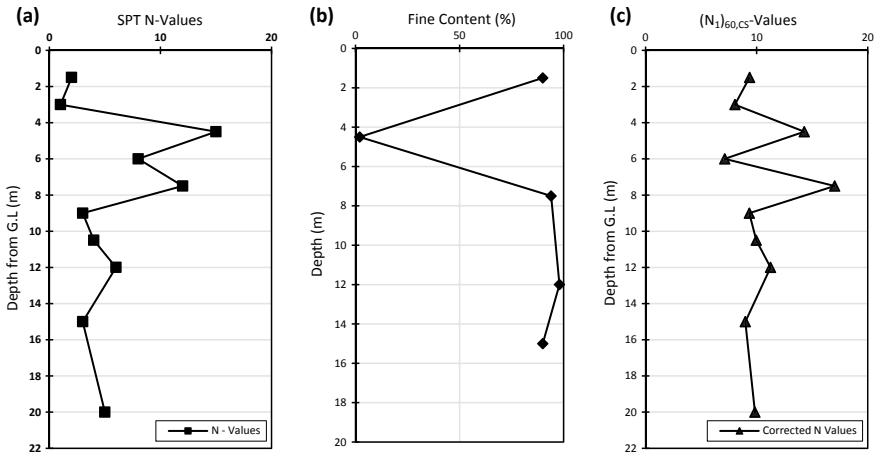
Fig. 27.2   a SPT N-values of each layer with increasing depth from the ground level, **b** fine content in percentage for each layer, **c** corrected SPT $(N_1)_{60,CS}$ values varying with depth

the grain size criterion: susceptible to liquefaction, not susceptible and cases where further studies are required to draw solid conclusions. Skempton [19] launched a parameter known as the Activity (*A*) of the soil given as the ratio of plasticity index (PI) to the percentage of clay-size particles (2 μm). It is seen that both activities, along with particle size, are insufficient to predict soil behaviour from field observations on ground failure.

Boulanger and Idriss [6] proposed behaviour of fine-grained soil under categories of clay-like, intermediate, and sand-like behaviours. An A-line was plotted on experimental investigations, which depicted soils behaving differently under shear loadings

Table 27.2 Layer wise liquefaction susceptibility

Depth (m)	Liquefaction susceptibility
1.5	No
3	Yes
4.5	Yes
6	Yes
7.5	No
9	No
10.5	No
12	–
15	–
20	No

considering liquid limit and plasticity index. In general practice, soils having PI ≥ 7 can be safely considered to behave as clays. CL-ML soils with PI values ranging from 3–6 show intermediate behaviour but may have greater cyclic strength than non-plastic fine-grained soil at the same tip resistance. Any soil not complying with the above criteria can be classified under sand-like behaving soils. While it is also suggested to discard the use of Chinese susceptibility criteria possibly, Bray [7], on the other hand, came up with factors to determine liquefiability of soil based on the variation of plasticity of fine-grained soils with the ratio of water content to the liquid limit of soils (wc/LL). Three classifications – susceptible (wc/LL > 0.85 and PI < 12), moderately susceptible (wc/LL > 0.8 and PI < 18), and non-susceptible (PI > 18) were proposed for soils. Table 27.2 shows the liquefaction susceptibility for the fine-grained soil layers in the borehole considered for this study.

Standard Penetration Corrections

Bozorgnia and Bertero [4] tells us that with increasing density of soil the requisite threshold energy to trigger liquefaction, increases. Although the correlation between excess pore water pressure generated and energy are soil specific, the level of liquefaction triggering Arias intensity is evaluated by empirical relation to penetration resistance. From case studies with liquefaction and non-liquefaction, Kayen and Mitchell [10] provided a chart depicting the variation of threshold Arias intensity as a function of $(N_1)_{60}$, as shown in Fig. 27.3. Singnar and Sil [18] showed that the correction for measured SPT values in the field are needed to be corrected based on a certain array of factors, such as, overburden pressure (C_N), hammer efficiency (C_E), borehole diameter (C_B), rod length (C_R), and sampler with or without liner (C_S). The observed SPT values are corrected for approximately 100 kPa of overburden pressure, and is given in Eq. (27.3).

Fig. 27.3 Liquefaction chart based on Arias Intensity as given by Kayen and Mitchell [10]
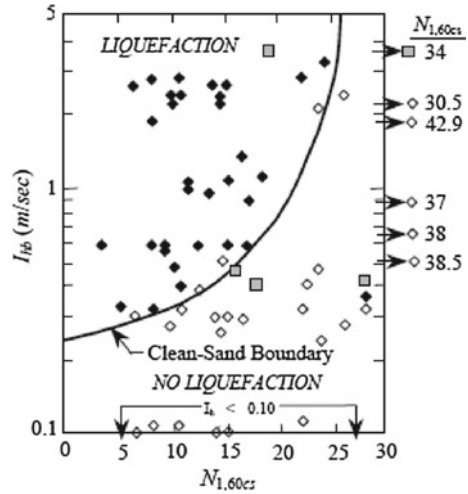
$$(N_1)_{60} = N_m \times C_N \times C_E \times C_B \times C_R \times C_S \tag{27.3}$$

In this case, N_m stands for the observed SPT N–count from field investigation and $(N_1)_{60}$ denotes the preliminary corrected Singnar and Sil [18], and Das et al. [8] adopted the relations to evaluate the overburden correction factor C_N as given by Liao and Whitman [13]. This paper adopts the following expression to calculate the overburden correction factor demonstrated by Kayen et al. [11] in Eq. (27.4).

$$C_N = \frac{2.2}{\left(1.2 + \frac{\sigma'_{vo}}{P_a}\right)} \tag{27.4}$$

Here, σ'_{v0} represents the effective overburden stress at the soil strata where the SPT value is being considered and P_a is the atmospheric pressure taken as a value of reference.

Following Das et al. [8], the other correction factors C_E, C_B, and C_S are assigned 0.75, 1.05, and 1.0, respectively. Although the correction factor for rod length (C_R) adopts the value of 0.75 since the possible depth of liquefaction susceptibility at the concerned site is less than 3 m. Since sands having high silt content are generally observed to have a lower standard penetration tip resistance than clean sands with equivalent capacity of liquefaction prevention, the correction for fine content is provided as:

$$(N_1)_{60,CS} = (N_1)_{60,SS} + \Delta N_1 \tag{27.5}$$

$(N_1)_{60,CS}$ = SPT resistance value equivalent to clean sand, $(N_1)_{60,SS}$ = SPT resistance of silty sand and ΔN_1 = correction factor for content of fine particles (FC). The value of ΔN_1 is determined by the fine content of the soil as per the

following conditions given in Eq. (27.6).

$$\Delta N_1 = \begin{cases} 0 & \text{for} & FC \leq 5\% \\ \frac{7}{30}(FC - 5) & \text{for } 5\% < FC < 35\% \\ 7 & \text{for} & FC \geq 35\% \end{cases} \tag{27.6}$$

Liquefaction Potential Analysis

The factor of safety (F_S) of the soil against liquefaction is defined as the ratio of capacity to demand of the soil in terms of energy. In this work, capacity is the threshold Arias intensity needed to trigger the liquefaction, and demand holds the value of Arias intensity developed during the scenario earthquake. The chart below (Fig. 27.3) by Kayen and Mitchell [10] gives the triggering intensity of liquefaction ($I_{hb,eq}$) as derived from various case studies based on corrected $(N_1)_{60,CS}$ values. The curved line represents the clean sand boundary for $I_{hb,eq}$ values as a function of corresponding resistances to penetration of the potentially liquefiable soil in the subsurface profile.

Results and Discussion

In this paper, evaluation of Liquefaction Potential Index (LPI) is attempted using the Arias intensity approach. Iwasaki et al. [9] categorized liquefaction damage by the severity of liquefaction. He devised the parameter called LPI to address the severity of liquefaction of an area based on the Factor of Safety (F_S) against the geohazard. Moreover, Iwasaki et al. [9] ruled out the category of moderate liquefaction in his study and considered only the possibility of low and high liquefaction. Sonmez [20] modified the LPI and the liquefaction potential categories to overcome the shortcomings given above. Due to involvement of geological and seismological criteria for liquefaction analyses, the uncertainties accompanying the fines content and the SPT values cannot be ignored. While Ulusay and Kuru [21] proposed $F_S = 1.2$ as the triggering value for marginally liquefiable and non-liquefied soils, $1.25 \leq F_S \leq 1.5$ are considered acceptable by Seed and Idriss [18]. Hence, Sonmez [20] took up 1.2 as the least value for non-liquefied category and devised the following LPI evaluation procedure:

$$\text{LPI} = \int_0^{20} W(z) F(z) \, \mathrm{d}z \tag{27.7}$$

Proposed by Iwasaki [9], $W(z)$ is expressed as a function of depth $= z$ and given as:

$$W(z) = 10 - 0.5z \tag{27.7a}$$

The term $F(z)$ is expressed in terms of the factor of safety at the desired depth z.

$$F(z) = \begin{cases} 1 - F_S & \text{for} \quad F_S \leq 0.95 \\ 2 \times 10^6 \times e^{-18.427 F_S} & \text{for } 0.95 < F_S < 1.2 \\ 0 & \text{for} \quad F_S \geq 1.2 \end{cases} \tag{27.7b}$$

Since the GWT is located at a depth of approximately 2.15 m below the ground level, the soil above the level of commencement of the water table is considered non-liquefiable. As per Boulanger [6], in this study, it was found that the plasticity index for the dark grey soft sandy clayey silt fell within the range of 4 to 5 and when reduced by a point or two, the CL-ML soil converts to ML and it behaves like a sand. For a further sense of validation of the results, the layer was tested according to the susceptibility criteria proposed by Bray [7], and according to the parameters the soil falls within the 'susceptible' zone. Hence, for the remaining depth within the water table the soil has been considered to be liquefiable.

Sonmez [20] considered a constant factor safety for the total soil column up to an excavated maximum depth of 20 m. In this paper, the factor of safety has been calculated for each soil stratum. F_S values are calculated for the thickness of each soil layer that has been regarded for this study and subsequently liquefaction potential has been calculated individually which layer sums up to an average LPI value for the entire borehole. That said, the limits in the integral given in Eq. (27.7) vary from layer to layer. The categorization of LPI as provided by Sonmez [20] is given in Table 27.3.

Hence, the liquefaction potentials for all the layers in the borehole cross-section has been given in Table 27.4. From depth 10.5 to 20 m, the soil layers are found to be non-susceptible to liquefaction as mentioned earlier. Hence the LPI for the last two strata are ignored in this study since they have no contribution towards the liquefiability of the soil profile. The light grey soft to medium clayey silt as per Andrews and Martin [2] is not susceptible because it has a clay content of 32%, whereas, the liquid limit is 32.5%. Cross-verified with criteria proposed by Boulanger

Table 27.3 Modified liquefaction potential classification proposed by Sonmez [20]

LPI	Factor of Safety (F_S)	Liquefaction potential
0	$F_S \geq 1.2$	Not liquefied
$0 < LPI \leq 2$	$1.2 > F_S \geq 1$	Low
$2 < LPI \leq 5$	$1 > F_S \geq 0.95$	Moderate
$5 < LPI \leq 15$	$0.95 > F_S \geq 0.85$	High
$LPI > 15$	$F_S < 0.85$	Very high

Table 27.4 Classification of BH-02 sample layers based on the liquefaction potentials

Depth	r_b	$I_{h,eq}$	$I_{h,l}$	F_S	LPI	Average LPI
1.5	0.86	1.08	0.55	0.51	0	4.16
3	0.74	0.93	0.5	0.54	8.53	
4.5	0.64	0.81	0.7	0.87	1.88	
6	0.56	0.70	0.4	0.57	6.21	
7.5	0.50	0.62	0.8	1.29	–	
9	0.45	0.56	0.55	0.99	–	
10.5	0.40	0.51	0.6	1.19	–	
12	0.37	0.47	0.6	1.28	–	
15	0.34	0.42	0.52	1.24	–	
20	0.34	0.42	0.55	1.30	–	

[6], the soil has a plasticity index higher than 7 and hence confidently depicts a clay-like behaviour. Both of the tests show non-susceptibility to liquefaction and hence is not considered in this study. The last layer of light grey firm clayey silt in the borehole cross-section exhibits a clay-like behaviour as well supported by its Atterberg parameters and hence is ignored.

From Table 27.4 it is evident that the borehole (BH - 02) represents a moderately liquefiable soil profile taking into account all the soil strata at the location. Figure 27.4a exhibits the curves showing the fluctuation of F_S with increasing depth from the ground level and (b) shows Liquefaction Potential Indices of different layers of the borehole.

Conclusions

In this deterministic approach, going by the liquefaction potential classifications proposed by various researchers, it is not ultimate to believe that if the soil exceeds a specific range of values, then liquefaction may be moderate, high or low as the case may be. The liquefaction of soil is determined by the frequency of earthquake loading and even the duration for which the ground shakes. In the context of the present study, considering an earthquake event of a fixed magnitude having a particular frequency and duration content, the area under target is 'moderately' liquefiable. For higher magnitude earthquakes, the same region may be highly liquefied with a considerable duration of ground shaking. Nevertheless, this study proves the efficacy of an energy-based approach towards a deterministic evaluation of liquefaction, and the results are congruent since slight liquefaction phenomena are reportedly sighted at this place after the seismic event. Hence, it can be safely noted that Arias intensity approach shines as a liquefaction potential analysis mechanism using the acceleration time history of an earthquake without the hassle of scaling the magnitudes as done for
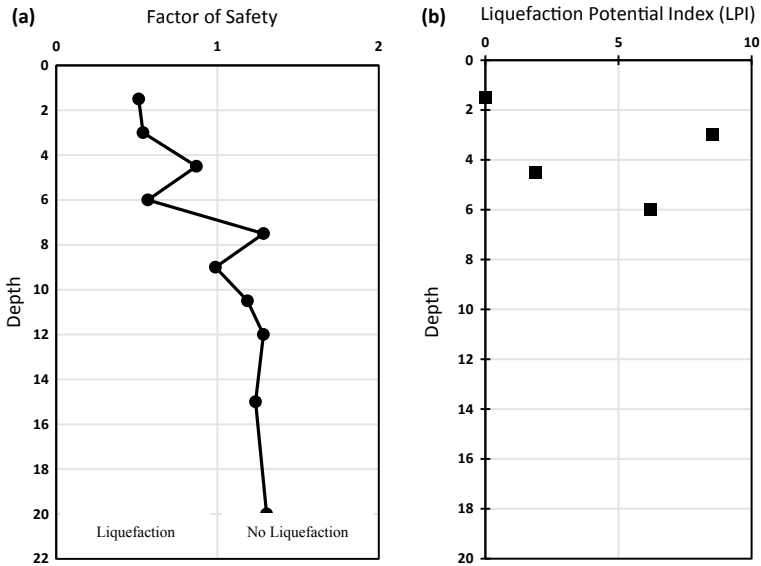
Fig. 27.4 a Variation of Factor of safety (F_S) with depth considering the entire cross-section of borehole, **b** Liquefaction Potential Index (LPI) values for the liquefiable layers

the stress-based approaches. A probabilistic evaluation can further be carried out to study liquefaction's recurrence rate at a previously liquefied location.

References

1. Anbazhagan P, Mog K, Nanjunda Rao KS, Siddharth Prabhu N, Agarwal A et al (2019) Reconnaissance report on geotechnical effects and structural damage caused by the 3 January 2017 Tripura earthquake, India. Nat Hazards 425–450. https://doi.org/10.1007/s11069-019-03699-w
2. Andrews DA, Martin GR (2000) Criteria for liquefaction of silty soils. In: 12th world conference on earthquake engineering. NZ Soc. for EQ Engrg, Upper Hutt
3. Arias A (1970) A measure of earthquake intensity. In: Press M (ed) Seismic design for nuclear power plants, pp 438–483
4. Bertero VV, Bozorgnia Y, Bolt BA, Campbell KW, Bertero RD (2004) Earthquake engineering from engineering seismology to performance-based engineering. Taylor & Francis, New York
5. Boulanger RW, Idriss IM (2004) Evaluating the potential for liquefaction or cyclic failure of silts and clays. University of California, Davis, California
6. Boulanger RW, Idriss IM (2006) Liquefaction susceptibility criteria for silts and clays. J Geotech Geoenviron Eng 132:1413–1426
7. Bray JD, Sancio RB (2006) Assessment of the liquefaction susceptibility of fine-grained soils. J Geotech Geoenviron Eng 132:1165–1177

8. Das S, Ghosh S, Kayal JR (2018) Liquefaction potential of Agartala City in Northeast India using a GIS platform. Bull Eng Geol Env. https://doi.org/10.1007/s10064-018-1287-5

9. Iwasaki T, Tokida K, Tatsuoka F, Watanabe S, Yasuda S, Sato H (1982) Microzonation for soil liquefaction potential using simplified methods simplified methods. In: 3rd international conference on microzonation, vol 3, Seattle, pp 1319–1330

10. Kayen RE, Mitchell JK (1997) Assessment of liquefaction potential during earthquakes by Arias Intensity. J Geotech Geoenviron Eng 1162–1174

11. Kayen RE, Mitchell JK, Seed RB, Lodge A, Nishio S, Coutinho R (1992) Evaluation of SPt-, CPT-, and shear wave based methods for liquefaction potential Assessment using Loma Prieta Data. In: 4th Japan-US workshop on earthquake-resistant design of lifeline fac. and countermeasures for soil liquefaction, vol 1, pp 177–204

12. Lee KL, Chan K (1972) Number of equivalent significant cycles in strong motion earthquakes. In: International conference on microzonation, vol II. Seattle, WA, pp 609–627

13. Liao S, Whitman RV (1986) Overburden correction factors for SPT in sand. J Geotech Eng 112:373–377

14. Nemat-Nasser S, Shokooh A (1979) A unified approach to densification and liquefaction of cohesionless sand in cyclic shearing. Can Geotech J 16:649–668

15. Parvez IA, Magrin A, Vaccari F, Mir RR, Peresan A, Panza GF (2017) Neo-deterministic seismic hazard scenarios for India—a preventive tool for disaster mitigation. J Seismol. https://doi.org/10.1007/s10950-017-9682-0

16. Seed HB, Idriss IM (1971) Simplified procedure for evaluating soil liquefaction potential. J SoilMech Found Div 1249–1274

17. Seed HB, Idriss IM (1982) Ground motions and soil liquefaction during earthquakes. Earthquake Engineering Research Institute

18. Singnar L, Sil A (2017) Assessment of liquefaction potential of Guwahati city based on geotechnical standard penetration test (SPT) data. In: Disaster advances, pp 10–21

19. Skempton AW (1953) The colloidal activity of clay. In: Proceedings of the 3rd international conference on soil mechanics and foundation engineering, vol 1, pp 57–61

20. Sonmez H (2003) Modification of the liquefaction potential index and liquefaction susceptibility mapping for a liquefaction-prone area (Inegol, Turkey). Environ Geol 44:862–871. https://doi.org/10.1007/s00254-003-0831-0

21. Ulusuay R, Kuru T (2004) 1998 Adana-Ceyhan (Turkey) earthquake and a preliminary microzonation based on liquefaction potential for Ceyhan town. Nat Hazards 32(1):59–88. https://doi.org/10.1023/B:NHAZ.0000026790.71304.32

22. Youd TL, Idriss IM (2001) Liquefaction resistance of soils: summary report from the 1996 Nceer and 1998 Nceer/Nsf workshops on evaluation of liquefaction resistance of soils. J Geotech Geoenviron Eng 127:297–313